J Polym Environ (2017) 25:692–700
DOI 10.1007/s10924-016-0854-8

ORIGINAL PAPER

Preparation and Fundamental Characterization of Cellulose Nanocrystal from Oil Palm Fronds Biomass

Rudi Dungani[1] · Abdulwahab F. Owolabi[2,3] · Chaturbhuj K. Saurabh[2] · H. P. S. Abdul Khalil[2,4] · Paridah M. Tahir[4] · C. I. C. M. Hazwan[2] · Kamoldeen A. Ajijolakewu[2,3,5] · M. M. Masri[2] · E. Rosamah[6] · P. Aditiawati[1]

Published online: 5 October 2016

Abstract The objective of this work was to isolate cellulose nanocrystal (CNC) from oil palm fronds (*Elaeis guineensis*) and its subsequent characterization. Isolation involves sodium hydroxide/anthraquinone pulping with mechanical refining followed by total chlorine free bleaching (includes oxygen delignification, hydrogen peroxide oxidation and peracetic acid treatment) before acid hydrolysis. Bleaching significantly decreased kappa number and increased α-cellulose percentage of fibers as confirmed by Technical Association of the Pulp and Paper Industry standards. Transmission electron microscopy (TEM), X-ray diffraction, Fourier transform infrared spectroscopy and thermogravimetric analysis revealed that acid hydrolysis along with bleaching improved crystallinity index and thermal stability of the extracted nanocrystals. It was observed that CNC maintained its cellulose 1 polymorph despite hydrolysis treatment. Mean diameter as observed by TEM and average fiber aspect ratio of obtained CNC was 7.44 ± 0.17 nm and 16.53 ± 3.52, respectively making it suitable as a reinforcing material for nanocomposite.

Keywords Nanocrystalline cellulose · Total chlorine free bleaching · Oil palm fronds · Thermal properties · X-ray diffraction · Fourier transform infrared spectroscopy

Introduction

Recently non-conventional fiber plants such as lignocellulosic agricultural by-products are used for the extraction of nano cellulose. Studies have been focused on such non-conventional agricultural residues for nano cellulose production with potential applications and this promotes the exploitation of underutilized plant fibers such as oil palm fronds. Global demand and supply of oil palm have drastically increased in recent decades due to the rise of various products among its chain of multiple uses [1]. In Malaysia growth in oil palm plantation has resulted in corresponding increase in the generation of oil palm biomass waste which include oil palm trunk, oil palm empty fruit bunches, palm oil mill effluent, and oil palm fronds (OPF) of which OPF constitute 70 % (w/w) of total biomass waste [2]. The continuous accumulation of this waste especially OPF at plantation sites is a potential threat to our ecosystem due to the production of greenhouse gases during microbial degradation. Oil palm biomass has been extensively analysed in the context of its rich physicochemical properties, economic advantage and enormous variety of biomass it generates [3–5]. On the basis of all these attributes the waste generated from oil palm biomasses are suitable for use in pulp, paper and production of extracted fibers. They

✉ Chaturbhuj K. Saurabh
chaturbhuj_biotech@yahoo.co.in

1 School of Life Sciences and Technology, Gandung Labtex XI, Institut Teknologi Bandung, Bandung, Indonesia

2 School of Industrial Technology, Universiti Sains Malaysia, 11800 Penang, Malaysia

3 Federal Institute of Industrial Research Oshodi, Lagos, Nigeria

4 Laboratory of Biocomposite Technology, Institute of Tropical Forestry & Forest Products, University Putra Malaysia, Selangor, Malaysia

5 Department of Microbiology, University of Ilorin, Ilorin, Nigeria

6 Faculty of Forestry, Mulawarman University, Campus Gunung Kelua, Samarinda 75119, East Kalimantan, Indonesia

are also a source of raw materials to some small scale industries which converts them into fertilizer, mattress filling, medium density fibreboard and composite material [6]. Recently, papermaking plant was commissioned in Malaysia by Eko Pulp and Paper Industries in collaboration with Forestry Research Institute Malaysia (FRIM) to produce printing paper from empty fruit bunches. However, of all the biomass waste generated from oil palm plantation sites industrial use of OPF has not been adequately explored. OPF can be a good source of reinforcement in bio-composite. Potential use of OPF as a source for natural cellulose fibers will boost the economy of farmers and eliminate the problem of massive biomass disposal. These cellulose fibers can be used for the production of cellulose nanocrystal (CNC).

CNC is biodegradable and gaining increasing interest in bio-composite formulations because of its renewability and ease of production. It can be used in nanocomposites as fillers, reinforcing component or network matrix. CNC makes tremendous impact on various properties of composite material due to its ability to form stable cross linked network in matrices [7]. Most commonly used procedures for the production of CNCs are acid hydrolysis of microfibrillated cellulose obtained from 2,2,6,6-tetramethylpiperidine-1-oxyl radical (TEMPO) mediated oxidation of fibrillated cellulose and ultrasonication of microcrystalline cellulose. Acid hydrolysis of native cellulose involves the cleavage of disordered or paracrystalline domains in cellulose chains. This is ascribed to the kinetics dissimilarities of hydrolysis of amorphous and crystalline realms [8]. It is well known fact that the amorphous or paracrystalline domains are more susceptible to acid attack in contrast to crystalline regions. Acid hydrolysis is expected to generate homogeneous crystallites. Prior to hydrolysis samples are beached to increase the crystallinity of cellulose by removal of amorphous hemicellulose from the biomass and thus improves the quality of dissolving pulp used for CNC production [9]. There are various reports on isolation of CNC from non-conventional agricultural waste which include pineapple leaf fibers [10], Sweden root [11], grass [12], rice husk [13, 14], rice straw [15] etc. Furthermore, the use of empty fruit bunches for CNC has also been reported [16–18]. Recently, Lamaming et al. 2015 [19] reported the isolation of CNC from an oil palm trunk using chemo-mechanical process. However, to the best of our knowledge no study on CNC isolated from OPF has been published using total chlorine free bleaching (TCF). The main advantage of TCF is that the use of harmful chlorine is totally avoided for the production of CNC thus turning the isolation procedure eco-friendly.

In present study CNC was isolated from OPF and its subsequent morphology was evaluated through field emission scanning electron microscope (FESEM) and transmission electron microscope (TEM). In present study chlorine free bleaching was used for CNC isolation to reduce the environmental hazard. The screen yield (%), kappa number, alpha cellulose and pulp viscosity were obtained according to Technical Association of the Pulp and Paper Industry (TAPPI) standard. Thermal properties of isolated CNC were characterised using thermogravimetric analysis (TGA) and functional groups were determined by using Fourier transform infrared (FT-IR) spectroscopy, however, crystallinity index was calculated by X-ray diffraction (XRD) analysis.

Experimental

Sample Preparation

OPF were obtained from oil palm plantation in Balik Pulau (Penang, Malaysia) and shredded followed by drying at 30 °C for 72 h. Dried fronds were cut into a size of 2 × 2 cm and subsequently grounded to smaller size using a Willey Mill (IKA MF10, Japan) and screened with a 500 µm aluminium sieve prior to storage in plastic bag. All chemicals used including sodium hydroxide pellet (98 %), sulphuric acid (98 %), hydrogen peroxide (30 %), acetic acid (98 %) and anthraquinone (AQ) were of laboratory grade.

Isolation of Cellulose Fiber

Isolation of cellulose commenced with the treatment of OPF at 1:10 (w/v) fibre to water ratio in a locally fabricated stainless steel 5 L cylindrical mini-digester at 160 °C for 30 min. Subsequently, soda-AQ pulping of 200 g of OPF was carried out at liquid (aqueous solution containing 25 % (w/w) soda concentration and 0.1 % (w/w) anthraquinone) to fiber ratio of 7:1 (v/w) and temperature was set at 160 °C for 120 min. Later, the obtained OPF pulp fibers were disintegrated using locally fabricated 50 L stainless steel hydro-pulper followed by washing and screening using 200 mesh screen size. Acquired pulp was subjected to mechanical refining using sprout Bauer twin disc 10″ refiner subsequently dewatered and oven dried at 105 °C for 1 h. Obtained dried pulped fiber was stored till further analysis. Screen yield was determined gravimetrically and kappa number was determined by TAPPI standard T236 om-85. Pulp viscosity and alpha cellulose was determined by capillary viscometer method (TAPPI standard T230 om-94) and TAPPI test method T203, respectively.

Total Chlorine Free (TCF) Bleaching

100 g of oven dried isolated pulped fiber was bleached. It involves oxygen delignification, hydrogen peroxide

oxidation and peracetic acid oxidation. Soda-AQ extracted fibers undergone for oxygen delignification in a 5 L stainless steel oxygen delignification vessel equipped with stirrer. OPF pulp was premixed with 1 % (w/v) $MgSO_4$, 2.5 % (w/v) NaOH, 0.02 % (w/v) AQ and 1.5 % (w/v) H_2O_2 and charged into the bleaching chamber. Process continued for 30 min at 95 °C and 80 Psi pressure. Obtained pulp was thoroughly washed and drained followed by second treatment using peracetic acid (PAA) (prepared in situ). The in situ preparation of PAA involved the combination of acetic acid and hydrogen peroxide in ratio of 1:5 (v/v). This process involved the oxidation of pulp using 0.5 mL of prepared PAA at 10 % (w/v) having pH 5. The reaction mixture was packed into transparent polyethylene bags and put into a water bath at 70 °C for 15 min with continuous kneading during the reaction. At the end of the reaction pulps were washed thoroughly with distilled water and drained. Finally the pulp was made to pass through the third treatment. Sample was pre-mixed with 1 % (w/v) $MgSO_4$, 2.0 % (w/v) NaOH, 0.02 % (w/v) AQ and 1.2 % (w/v) H_2O_2 followed by feeding the mixture into bleaching plant and the reaction was set at 95 °C for 30 min at 80 Psi pressure. The bleached pulp was washed, drained and dried at 105 °C for 1 h.

Acid Hydrolysis

40 g of oven dried bleached OPF fibers were subjected to acid hydrolysis by using 8.75 mL of a sulphuric acid per gram of bleached pulp at 45 °C with continuous stirring for 15 min. Later 400 mL of cold distilled water was added and mixture was kept overnight at 30 °C further the clear supernatant was decanted. Hydrolyzed fibers were washed with cold distilled water repeatedly until neutrality at constant pH was reached. The acid was finally removed by centrifugation at 4000 rpm at 30 °C for 10 min followed by dialysis using membrane of regenerated cellulose with distilled water for 72 h until pH of neutrality reached. Prepared OPF-CNC was then homogenised by sonication before analysis.

Surface Morphology Characterization

Surface morphology characterization of all samples was carried out using FESEM. The structural transformation was examined on Leo Supra 50 VP Field Emission equipped with Oxford INCA-X energy dispersive microanalysis system (Carl Zeiss, Yokohama, Japan). Prior to analysis each sample was gold-sputtered using sputter coater model Polaron SC (Hertfordshire, England) with 515 ± 20 nm sample size thickness..

TEM Analysis

The structural dimensions of OPF-CNC were observed under high resolution TEM using a Philips CM 12 (Japan) electron microscope with an accelerating voltage of 80 kV. A drop of 0.1 wt% of OPF-CNC suspensions was placed on copper grids coated with a carbon support film for observation. The specimens were stained with a small drop of 2 % uranyl acetate to improve the viewing contrast while excess liquid stain on the copper grid surface was removed with a small piece of filter paper by lightly touching the edge of copper grid. A total of 20 OPF-CNC's dimensions were measured and result was reported as the mean value of data from each set of measurements.

FT-IR Analysis

Possible changes in functional group were monitored with FT-IR spectroscopy. 1 mg of each sample was pulverised and mixed with 99 mg of KBr and resultant mixture was introduced into a hollow chamber and pressed to make a small pellet. The pellet was run on a Nicolet infrared spectrophotometer (Avatar 360 FT-IR E.S.P, Massachusetts, USA). The prepared pellet was scanned 64 times in spectra transmittance region between wave numbers 4000 to 500 cm^{-1} at 4 cm^{-1} resolution at 30 °C.

XRD Analysis

Crystallinity of the sample was monitored by XRD with Ni-filtered CuKα radiation (wavelength of 1.5406 Å). The diffractometer was operated on 40 kV voltage and 40 mA current. Samples were scanned at 2° per minute with a 2θ angle range from 5° to 60°. The crystallinity index (*Crl*) value was calculated according to Segal et al. (1959) Eq. (1):

$$Crl(\%) = \frac{(I_{002} - I_{am})}{I_{002}} \times 100 \quad (1)$$

where I_{002} and I_{am} are the peak intensity corresponding to crystalline and the amorphous fraction of cellulose respectively.

The average crystallite size was calculated from the Scherrer Eq. (2) based on the crystalline region.

$$D_{002} = \frac{k\lambda}{B_{002}\cos\theta} \quad (2)$$

where D_{002} represents the crystal size (nm) of cellulose I structure in respect of (002) plane, k is the Scherrer constant (0.84), λ is the X-ray wavelength (1.54 Å), B (in radians) is full-width at half of the peak (FWHM) of I_{002} diffraction peak, and θ is the corresponding Bragg angle.

TGA

Thermogravimetric analysis (TGA) of the samples was carried out on Perkin-Elmer TGA 7 (Massachusetts, USA) with temperature ranging from 30 to 800 °C at a heating rate of 10 °C/min. Heating of sample was carried out under nitrogen atmosphere to prevent any thermoxidative degradation. A 9 mg of the sample was loaded onto TGA to determine its thermal decomposition. Furthermore, residual char obtained at 500 °C.

Particle Size and Stability Measurement

The NCC suspension (0.05 wt%) was sonicated for 5 min in an Grant Instruments MXB ultrasonic baths (UK) equipped using 40 kHz of ultrasound frequency, 135 W RMS power. Later, zeta potential was determined using a Zetasizer Nano Z model ZEN 2600 (Malvern Instruments, UK). The particle size was measured using the Smoluchowski algorithm. Each value was obtained by averaging the measurements of three samples.

Elemental Analysis

The elemental analysis was carried out to investigate the total content of elements in isolated CNC from OPF by using CHNS-932 elemental analyser (LECO, USA). Carbon, hydrogen, nitrogen and sulphur content of nano cellulose were measured independently.

Result and Discussion

Fiber Characteristics

Effect of bleaching on the properties of pulped OPF fibers were presented in Table 1. It was observed that the bleaching significantly increased α-cellulose content of fibers as compared to pulped fiber (unbleached). Alpha cellulose has the highest degree of polymerization and is the most stable among all classes of cellulose. Observed improvement in α-cellulose content was attributed to the successive removal of all non-cellulosic materials from the OPF biomass leaving pure cellulose behind after bleaching. The kappa number estimates the amount of residual lignin content in the pulp. Lower kappa number in bleached OPF fiber than pulped fiber signifies the removal of non-cellulosic materials. Costa and Colodette [20] reported that as the number of bleaching cycle increases Kappa number reduces. Furthermore, elemental analysis was carried out to and it was confirmed that the sulphuric hydrolysis resulted in high percentage of observed sulphur concentration in CNC (Table 2).

Table 1 Characteristic of pulped and bleached OPF fiber

	Pulped OPF fibre	Bleached OPF fibre
Kappa number (K_n)	20.50 ± 0.4	7.58 ± 0.34
α-cellulose (%)	54.53 ± 0.4	96.50 ± 0.3
Viscosity (cP)	16.17 ± 0.05	11.23 ± 0.09

In TCF bleaching, oxygen bleaching was characterised by oxidative degradation of phenolic lignin which resulted in release of lignin–carbohydrate fragments [21–23] thus increase in α- cellulose percentage and decrease in kappa number was observed. Hydrogen peroxide which is site specific reacted with chromophoric portion of OPF through chemisorptions. However, in PAA oxidation reaction electrophilic hydroxylation, quinone formation, lactones and muconic acid formation occurred between lignin and PAA [24]. The degree of polymerisation is determined by the viscosity which decreased after bleaching. The reduction of viscosity from 16.17 ± 0.05 to 11.23 ± 0.09 cP for pulped and bleached OPF fibers, respectively, was attributed to secondary peeling in which alkaline hydrolyses the glycosidic linkages. The peeling reaction basically involves the decompression of carbohydrates from the aldehyde end removing one terminal sugar molecule at a time [25]. Alkaline treatment resulted in random cleavage of glycosidic bonds which led to lower the yield [26]. Screen yield of obtained OPF fiber in present study was 45.31 %.

Microstructure Analysis

SEM image of raw, pulped OPF fiber and OPF-CNC are displayed in Fig. 1. Raw fiber was composed of bundles that are bound together by cemented components of lignin, hemicelluloses and waxy materials which gave typically rough and irregular surface to raw fibers (Fig. 1a). Soda-AQ pulping led to removal of entire binding component of biomass like hemicellulose, pectin and lignin [27] which resulted in free cellulose fiber as shown in Fig. 1b.

Fiber morphology play important role in structural properties of composite materials [28]. Diameter of fiber is inversely proportional to its strength i.e. the smaller the diameter the higher will be its strength [29]. Pre-treatments like pulping, bleaching and acid hydrolysis significantly influence the CNC's dimensions [8]. TEM image revealed the needle shape like nanocrystal (Fig. 2). The image of the CNCs aqueous solution showed a cloudy or white suspension which was colloidally stable (Fig. 2). TEM measurement was used to determine the aspect ratio (length/diameter) of CNC. Length and diameter of CNC was found to be 106.33 ± 1.24 nm and 7.44 ± 0.17 nm, respectively (Table 2). Furthermore, aspect ratio plays a significant role in enhancing the chemical and physical

Table 2 Size, elemental analysis, and zeta potential of CNC derived from OPF

TEM (nm)		Aspect ratio	Elemental analysis (w/w%)				Zeta potential (mV)	Particle size (nm)
F.L	F.D		Carbon	Hydrogen	Nitrogen	Sulphur		
106.33 ± 1.24	7.44 ± 0.17	16.53 ± 3.52	46.26	5.59	0.26	2.56	−32.73 ± 2.04	62.27 ± 4.17

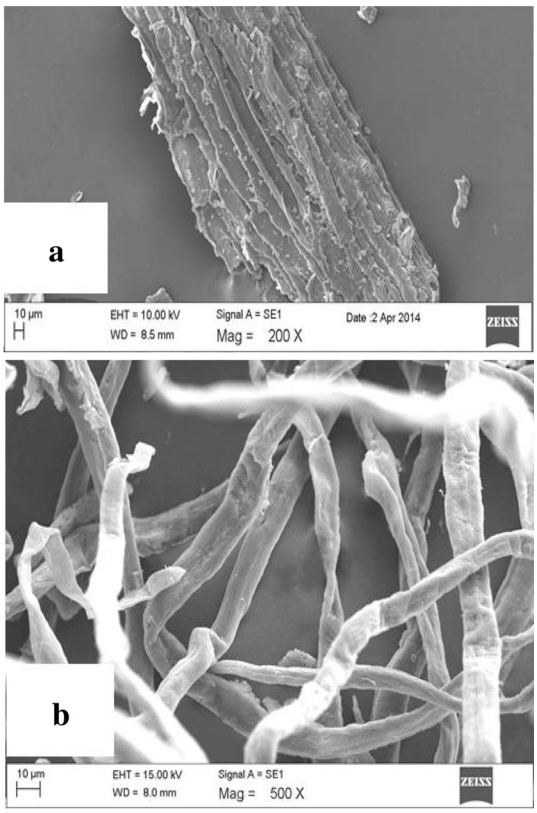

Fig. 1 Field emission scanning electron microscopy of **a** Raw OPF, **b** OPF pulp fibre

performances of CNC based polymer composite materials [30]. Higher aspect ratio resulted in better fiber-matrix adhesion which leads to improved functional properties [31]. The aspect ratio of obtained OPF-CNC was 16.53 ± 3.52 which is comparable with other non-conventional biomass based nano-materials. Aspect ratio of CNC derived from rice husk was 18 and from cotton fiber it was ranging between 10 to 14 [28, 32]. Thus it can be concluded on the basis of high aspect ratio of extracted CNC that it has the potential to be used as nanofiller for polymer matrices.

Thermal Analysis

Thermal analysis of all the samples is presented in Table 3; Fig. 3. It was observed that all the samples had initial weight loss between 5 and 6 wt% attributed to moisture loss. The second step of cellulose decomposition (T_{onset}) started at 202.83, 259.28 and 332.93 °C for raw fiber, pulped fibers and OPF-CNC respectively. Furthermore, the TGA results showed that the T_{max} (peak degradation temperature) of cellulose degradation for raw fiber, pulped fiber and CNC was 327.67 °C, 318.06 °C and 359.29 °C, respectively. It was observed that pre-treatments resulted in improved thermal stability of pulped fibers and OPF-CNCs as compared to raw fibers. Highest thermal stability of CNC was attributed to the subsequent removal of amorphous fraction of cellulose which includes hemicelluloses and lignin during soda-AQ pulping, bleaching and acid hydrolysis. Residual char of 24.3, 19.29 and 9.31 % were obtained for raw fiber, pulped fibers and OPF- CNC respectively. The char residue at the end of the heating was due to lignin [32]. Pre-treatment resulted in removal of lignin thus the lowest char residuse was from CNC.

The DTG curves in Fig. 3 displayed the loss of moisture or drying (denoted as "i") and active devolatization or loss of volatiles (denoted as "ii"). DTG result showed the presence of lower temperature peak at 290 °C for raw OPF fiber (Fig. 3) which corresponds to the decomposition of hemicellulose [33, 34]. Observed peak was shifted to higher temperature and remained as a shoulder for pulped fiber indicating partial removal of hemicellulose due to soda–AQ treatment. However, this peak was entirely absent in CNC indicating total removal of hemicellulose due to bleaching and acid hydrolysis.

X-ray Diffraction Analysis

XRD patterns of pulped fibers and CNC showed two peaks (marked as "i" and "ii") having typical characteristics of cellulose I polymorph (Fig. 4) [35]. Similarity in diffraction patterns of pulped fibers and OPF- CNC signifies the preservation of natural cellulose structure despite bleaching and acid hydrolysis. A sharp increase in intensity of OPF-CNC peak observed at 22.3° (marked as "ii") indicated an increase in purity of nanocrystals after acid hydrolysis (Fig. 4). Enhanced purity was a result of removal of non-cellulosic materials from nano cellulose. Crystallinity index of the pulped fibers and OPF- CNC were 70 and 78.5 % respectively. Increase in crystallinity was attributed to the removal of amorphous regions of cellulose during acid hydrolysis and subsequent hydrolytic cleavage of

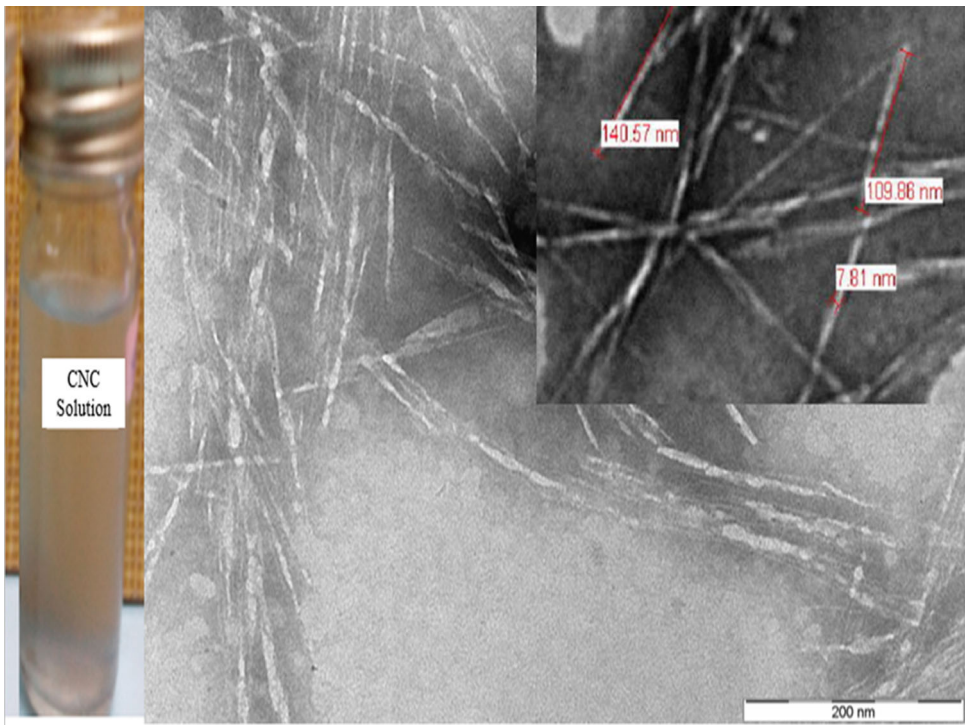

Fig. 2 TEM image of CNC (inserted with CNC solution and the measured image)

glycosidic bonds and releasing of individual crystallites [2].

The diameter of CNC from direct TEM measurement was found to be 7.44 ± 0.17 nm while from the Scherrer measurement it was 6.95 ± 0.17 nm. Both measurements showed a significant difference in OPF-CNC size this could be due to the thermal vibration of lattice sites in crystalline structure as explained by Debye thermal broadening [36].

FT-IR Spectroscopy

FT-IR spectra of raw fiber, pulped fiber and CNC are shown in Fig. 5. Observed spectra were dominated by a dip in the region between 3404.69 to 3412.96 cm^{-1} (marked as "i") which was assigned to stretching vibrations of -OH groups. The OH peak reflected the hydrophilic nature of major constituents of natural fibers such as cellulose, hemicelluloses and lignin [37]. Aliphatic saturated C-H stretching is indicated by the presence of another dip between 2901.83 to 2899.63 cm^{-1} (marked as "ii") which was assigned to methylene groups in cellulose [19]. Spectral band between 1734 to 1733 cm^{-1} (marked as "iii") was characteristic of ester linkage of carboxylic or acetyl and uronic ester groups. This peak was gradually reducing due to bleaching and hydrolysis treatment. Unique bands of ferulic and ρ-coumeric acids are found in an unconjugated carbonyl group which is typical characteristics of hemicelluloses [38]. This band (marked as "iii") was reduced after pulping and appeared as a shoulder which eventually disappeared after acid hydrolysis. Peak between 1432.34 to 1434.51 cm^{-1} (marked as "iv") correspond to C–C stretching vibrations of aromatic hydrocarbons of lignin ring [35]. Peaks from 1373.26 to 1325.22 cm^{-1} (marked as "v") were assigned to C–H asymmetric deformation of raw and pulped fibers, respectively. OPF-CNC sample demonstrated same peak at 1317 cm^{-1} which was attributed to CH_2 wagging cellulose characteristic of crystallised cellulose I polymorph [39].

Table 3 Thermal degradation profile of raw fibres, pulped fibers and OPF-CNC

Samples	Moisture removal			Cellulose degradation			Carbonic residue degradation			Char yield %
	T_{onset} (°C)	T_{max} (°C)	Weight loss (%)	T_{onset} (°C)	T_{max} (°C)	Weight loss (%)	T_{onset} (°C)	T_{max} (°C)	Weight loss (%)	
Raw fibres	30.00	77.00	5.41	202.83	327.67	26.57	539.17	658.21	43.72	24.3
Pulped fibres	30.00	84.80	5.21	259.28	318.06	40.74	540	720	34.76	19.29
OPF-CNC	30.00	84.80	6.16	332.93	359.29	58.71	735	797.67	25.82	9.31

T_{onset} is onset temperature, T_{max} is maximum degradation temperature

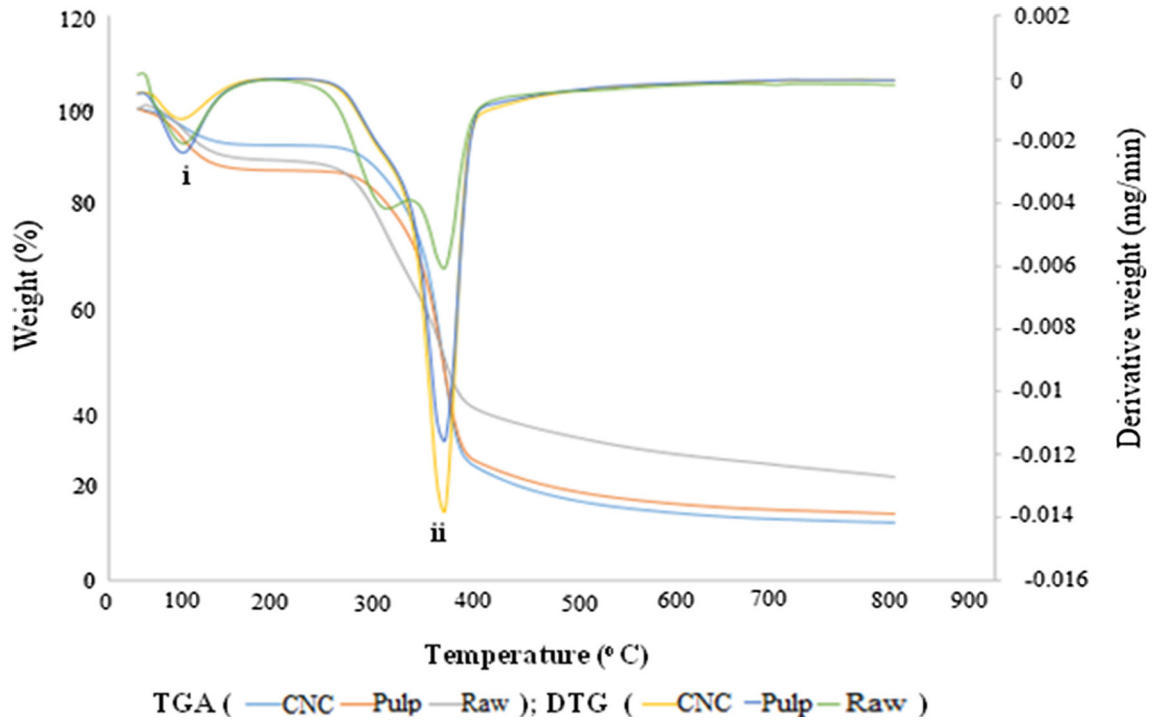

Fig. 3 TGA and DTG graph of raw OPF fibre, OPF-CNC, and extracted OPF pulp fibre

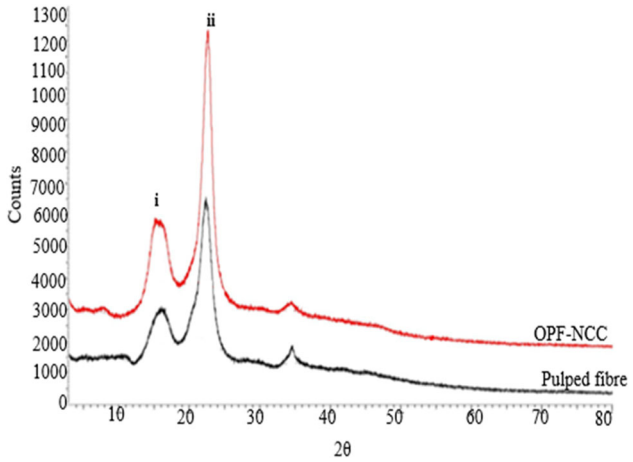

Fig. 4 XRD pattern of OPF-CNC and pulped fibre

Shifting of this peak in pulped fiber and CNC towards right as compared to raw fiber indicated the dissolution of lignin. Absent of peak at 1247 cm^{-1} in CNC (marked as "vi") showed that hemicellulose was removed from the produced nanocrystals. Observed transmittance band at 897.98 and 898.33 cm^{-1} (marked as "vii") was attributed to the β-glycosidic linkages of glucose units in cellulose and hemicellulose [39]. This reveals that the pulped fiber and CNC has high cellulose content. Intensity of this spectra increases with pre-treatment due the delignification of biomass as a result of soda-AQ pulping and bleaching. FT-IR analysis revealed the effectiveness of pre-treatment for removal of hemicellulose and lignin from CNC.

Particle Size Measurement and Zeta Potential

Table 2 shows the surface charge determined by the zeta potential and particle size of extracted nano cellulose. The large amount of sulphur percentage (2.56 %) and high zeta potential with a value of -32.73 ± 2.04 mV (Fig. 6) in OPF-CNC indicates incorporation of negatively charged sulphate groups into the cellulose chains during sulphuric acid hydrolysis. The colloidal stability was confirmed by analyzing zeta potential of CNC solution. The zeta potential value of colloidal dispersions if higher than 25 mV then suspension is considered very stable thus OPF-CNC suspension is considered stable [40].

Conclusion

This study demonstrated a novel method for obtaining CNC from OPF which is one of the most abundant waste biomass from oil plantation in Malaysia. Alkaline extraction of the OPF fiber in conjunction with total chlorine free bleaching resulted in higher crystallinity index, α-cellulose % and thermal stability of CNC as compared to raw fiber. Observed improvement was due to the various pre-treatment of raw OPF fiber before hydrolysis. XRD analysis further revealed

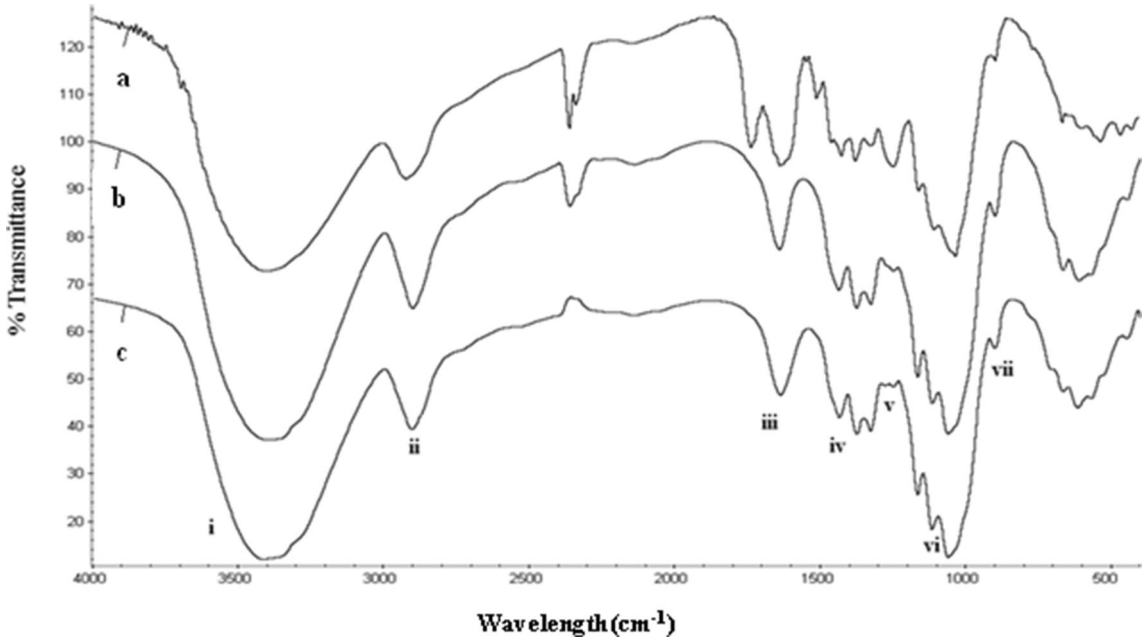

Fig. 5 FT-IR spectra of **a** Raw fibre, **b** Pulped fibres, **c** OPF-CNC

Fig. 6 Graph of apparent zeta potential of OPF-CNC (data in triplicates)

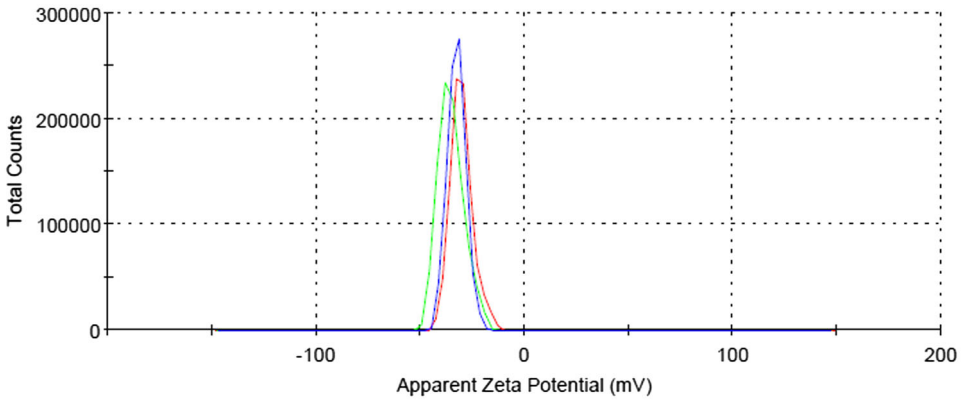

that these pre-treatments did not alter the typical characteristics of cellulose I polymorph. The aspect ratio of the OPF-CNC was 16.53 ± 3.52 which is comparable to already published data and crystallinity index was 78.5 % shows that the isolated nanocrystals has the potential to be used as a reinforcing agent for bio based nanocomposites.

Acknowledgments The authors would like to thank the Universiti Sains Malaysia for the awarded Postdoctoral Fellowship. The authors are gratefully acknowledged Universiti Sains Malaysia, Penang, Malaysia for providing Research University Grant (RUI-1001/PTE-KIND/814255).

References

1. Kopetz H (2007) Biomass–a burning issue: policies needed to spark the biomass heating market. Refocus 8(2):52–58
2. Owolabi AWT, Ghazali A, Wanrosli WD, Abbas FMA (2016) Effect of alkaline peroxide pre-treatment on microfibrillated cellulose from oil palm fronds rachis amenable for pulp and paper and bio-composite production. BioResources 11(2):3013–3026
3. Khalil HPSA, Mohamed SA, Ridzuan R, Kamarudin H, Khairul A (2008) Chemical composition, morphological characteristics, and cell wall structure of Malaysian oil palm fibers. Polym Plast Technol Eng 47(3):273–280
4. Khalil HPSA, Mohamed SA, Abdul KMO (2007) Chemical composition, anatomy, lignin distribution, and cell wall structure of Malaysian plant waste fibers. BioResources 1(2):220–232
5. Awalludin MF, Sulaiman O, Hashim R, Nadhari WNAW (2015) An overview of the oil palm industry in Malaysia and its waste utilization through thermochemical conversion, specifically via liquefaction. Renew Sust Energ Rev 50:1469–1484
6. Satyanarayana KG, Arizaga GG, Wypych F (2009) Biodegradable composites based on lignocellulosic fibers—an overview. Prog Polym Sci 34(9):982–1021
7. Khan A, Khan RA, Salmieri S, LeTien C, Riedl B, Bouchard J, Chauve G, Tan V, Kamal MR, Lacroix M (2012) Mechanical and

barrier properties of nanocrystalline cellulose reinforced chitosan based nanocomposite films. Carbohyd Polym 90(4):1601–1608
8. Habibi Y, Lucia LA, Rojas OJ (2010) Cellulose nanocrystals: chemistry, self-assembly, and applications. Chem Rev 110(6): 3479–3500
9. Chong YH, Daud WRW, Poh BT, Ibrahim M, Leh CP (2015) Application of photo, peracetic acid, and combination pre-treatments in improving totally chlorine-free bleaching selectivity. BioResources 10(3):4110–4125
10. Sheltami RM, Abdullah I, Ahmad I, Dufresne A, Kargarzadeh H (2012) Extraction of cellulose nanocrystals from mengkuang leaves (Pandanus tectorius). Carbohyd Polym 88(2):772–779
11. Hu Z, Cranston ED, Ng R, Pelton R (2014) Tuning cellulose nanocrystal gelation with polysaccharides and surfactants. Langmuir 30(10):2684–2692
12. Saritha S, Nair SM, Kumar NC (2013) Nano-ordered cellulose containing iα crystalline domains derived from the algae chaetomorpha antennina. BioNanoScience 3(4):423–427
13. Johar N, Ahmad I, Dufresne A (2012) Extraction, preparation and characterization of cellulose fibres and nanocrystals from rice husk. Ind Crop Prod 37(1):93–99
14. Dufresne A (2012) Processing of polymer nanocomposites reinforced with cellulose nanocrystals: a challenge. Int Polym Proc 27(5):557–564
15. Jan JS, Chen PS, Hsieh PL, Chen BY (2012) Silicification of genipin-cross-linked polypeptide hydrogels toward biohybrid materials and mesoporous oxides. ACS Appl Mater Interfaces 4(12):6865–6874
16. Fahma F, Iwamoto S, Hori N, Iwata T, Takemura A (2010) Isolation, preparation, and characterization of nanofibers from oil palm empty-fruit-bunch (OPEFB). Cellulose 17(5):977–985
17. Jonoobi M, Mathew AP, Oksman K (2012) Producing low-cost cellulose nanofiber from sludge as new source of raw materials. Ind Crop Prod 40:232–238
18. Haafiz MM, Eichhorn SJ, Hassan A, Jawaid M (2013) Isolation and characterization of microcrystalline cellulose from oil palm biomass residue. Carbohyd Polym 93(2):628–634
19. Lamaming J, Hashim R, Sulaiman O, Leh CP, Sugimoto T, Nordin NA (2015) Cellulose nanocrystals isolated from oil palm trunk. Carbohyd Polym 127:202–208
20. Costa MM, Colodette JL (2007) The impact of kappa number composition on eucalyptus kraft pulp bleachability. Braz J Chem Eng 24(1):61–71
21. Prez J, Munozorado J, de la Rubia TD, Martinez J (2002) Biodegradation and biological treatments of cellulose hemicellulose and lignin an overview. Int Microbiol 5(2):53–63
22. Leh CP, Rosli WW, Zainuddin Z, Tanaka R (2008) Optimisation of oxygen delignification in production of totally chlorine-free cellulose pulps from oil palm empty fruit bunch fibre. Ind Crop Prod 28(3):260–267
23. Munk L, Sitarz AK, Kalyani DC, Mikkelsen JD, Meyer AS (2015) Can laccases catalyze bond cleavage in lignin? Biotechnol Adv 33(1):13–24
24. Parida KN, Moorthy JN (2015) Synthesis of o-carboxyarylacrylic acids by room temperature oxidative cleavage of hydroxynaphthalenes and higher aromatics with oxone. J. Org. Chem 80:8354–8360
25. Yoon DE, Hwang C, Kang NR, Lee U, Ahn D, Kim JY, Song HK (2016) Dependency of electrochemical performances of silicon lithium-ion batteries on glycosidic linkages of polysaccharide binders. ACS Appl Mater Interfaces 8:4042–4047
26. Wahlström RM, Suurnäkki A (2015) Enzymatic hydrolysis of lignocellulosic polysaccharides in the presence of ionic liquids. Green Chem 17(2):694–714
27. Chandra J, George N, Narayanankutty SK (2016) Isolation and characterization of cellulose nanofibrils from arecanut husk fibre. Carbohyd Polym 142:158–166
28. de Morais TE, Bondancia TJ, Teodoro KB, Corrêa AC, Marconcini JM, Mattoso LH (2011) Sugarcane bagasse whiskers: extraction and characterizations. Ind Crop Prod 33(1):63–66
29. Siqueira G, Bras J, Dufresne A (2008) Cellulose whiskers versus microfibrils: influence of the nature of the nanoparticle and its surface functionalization on the thermal and mechanical properties of nanocomposites. Biomacromolecules 10(2):425–432
30. Siqueira G, Tapin LS, Bras J, da Silva PD, Dufresne A (2010) Morphological investigation of nanoparticles obtained from combined mechanical shearing, and enzymatic and acid hydrolysis of sisal fibers. Cellulose 17(6):1147–1158
31. Subhedar PB, Parag RG (2014) Alkaline and ultrasound assisted alkaline pretreatment for intensification of delignification process from sustainable raw-material. Ultrason Sonochem 21(1):216–225
32. Rosa SM, Rehman N, de Miranda MI, Nachtigall SM, Bica CI (2012) Chlorine-free extraction of cellulose from rice husk and whisker isolation. Carbohyd Polym 87(2):1131–1138
33. Li MC, Wu Q, Song K, Lee S, Qing Y, Wu Y (2015) Cellulose nanoparticles: structure–morphology–rheology relationships. ACS Sustain Chem Eng 3(5):821–832
34. Moriana R, Vilaplana F, Karlsson S, Ribes A (2014) Correlation of chemical, structural and thermal properties of natural fibres for their sustainable exploitation. Carbohyd Polym 112:422–431
35. Rosa MF, Medeiros ES, Malmonge JA, Gregorski KS, Wood DF, Mattoso LH, Glenn G, Orts WJ, Imam SH (2010) Cellulose nanowhiskers from coconut husk fibers: effect of preparation conditions on their thermal and morphological behavior. Carbohyd Polym 81(1):83–92
36. Ciupină VI, Zamfirescu S, Prodan G (2007) Evaluation of mean diameter values using scherrer equation applied to electron diffraction images. Springer. Netherlands 231–237
37. Khalil HA, Yusra AI, Bhat AH, Jawaid M (2010) Cell wall ultrastructure, anatomy, lignin distribution, and chemical composition of Malaysian cultivated kenaf fiber. Ind Crop Prod 31(1):113–121
38. Neto WP, Silvério HA, Dantas NO, Pasquini D (2013) Extraction and characterization of cellulose nanocrystals from agro-industrial residue–Soy hulls. Ind Crop Prod 42:480–488
39. Lionetto F, Del SR, Cannoletta D, Vasapollo G, Maffezzoli A (2012) Monitoring wood degradation during weathering by cellulose crystallinity. Materials 5(10):1910–1922
40. Mirhosseini H, Tan CP, Hamid NSA, Yusof S (2008) Effect of Arabic gum, xanthan gum and orange oil contents on zeta-potential, conductivity, stability, size index and pH of orange beverage emulsion. Colloids Surf A 315:47–56